

1 **Title Page**

2 Genetic structure of Photosystem II functionality in rice unraveled by GWAS analysis

3

4 running title: GWAS of PSII functionality in rice

5

6 Authors:

7 ¹Juan Manuel Vilas juanmvilas@gmail.com

8 ²Estanislao Burgos burgosestanislao@gmail.com

9 ¹Maria Lucrecia Puig lucreciapuig@gmail.com

10 ³Jose Colazo colazo.jose@inta.gob.ar

11 ³Alberto Livore alivore@yahoo.com.ar

12 ¹Oscar Adolfo Ruiz ruiz@intech.gov.ar

13 ²Fernando Carrari carrarifernando@gmail.com

14 ¹Andrés Alberto Rodriguez andres.a.rodriguez@gmail.com

15 ¹Santiago Javier Maiale santiagomaiale@hotmail.com

16

17 ¹ UBI, INTECH, CONICET-UNSAM, Int. Marino Km 8, Chascomús, Pcia. Bs As., Argentina

18 ² IFIBYNE, FCEyN, CONICET-UBA, Ciudad Universitaria, CABA, Argentina

19 ³ EEA INTA Concepción del Uruguay, Ruta 39 Km 143, Concepción del Uruguay, Pcia. ER, Argentina

20

21 date of submission:

22

23 five figures; four tables; three supplemental figures; three supplemental tables.

24

25 Total words: 4983

26

27

28

29

30

31

32

33

34

35 **Highlight:**

36 The genetic structure of the Photosystem II functionality in rice was studied by using genome-wide
37 association through chlorophyll fluorescence.

38

39 **Abstract:**

40 Rice production is a particularly important crop for the half-world population. Therefore,
41 knowledge about which genes are implicated in the functionality of the Photosystem II, that are
42 still poorly explored could collaborate in the assisted selection of rice improving. In the present
43 study, we applied Genome wide Association Studies of PSII chlorophyll fluorescence under two
44 contrasting environmental conditions in 283 rice accessions highly diverse. A total of
45 110 significant association SNP-phenotype were observed, and 69 quantitative trait loci identified
46 with a total of 157 genes, of which 38 were highly significant, mapped spread out through rice
47 genome. These underlying regions are enriched in genes related to biotic and abiotic stresses,
48 transcription factors, Calvin cycle, senescence, and grain characters. The correlations analyses PSII
49 chlorophyll fluorescence parameters and some panicle characteristics found here suggest the
50 possibility of developing molecular markers to assist the breeding programs that improve
51 photosynthesis and yield in rice.

52

53 **Keywords:** Chlorophyll Fluorescence, Gene, Genome-wide association, Panicle, Rice, Single
54 nucleotide polymorphisms

55

56 **Abbreviations:** %In, calculated infertility percentage; %F, fertility percentage; GO, gene ontology;
57 GWAS, genome-wide association; NSP, number of spikelet per panicle; PN, panicle number; PSII,
58 photosystem II; PW, panicle weight; SNP, single nucleotide polymorphisms; WTG thousand grain
59 weight.

60 **1. Introduction:**

61 Asian rice (*Oryza sativa* L.) is one of the most important crops in the world and constitutes,
62 approximately, the main food of the three billion humans in countries of Asia, Africa, and Latin
63 America (Sasaki, 2005, FAO 2009).

64 This species is classified into five subpopulations namely: Indica, Aus, Aromatic, Tropical Japonica,
65 and Temperate Japonica (Garriset *al.*, 2005).

66 Rice breeding in the past has focussed on augmented the harvested index and solar radiation
67 capture, achieving a significant increase of yield across time.

68 This advanced was supported, mainly, to the modified ideotype in the green revolution and
69 improvement in agronomic practices.

70 Rice breeders have developed a new plant type, that improvement the past ideotype, adapting it
71 for direct seeding. This new plant type design is characterized by reduced tillering capacity, large
72 panicle size, lodging resistance, and specific arrangement of the three top leaves (Penget *al.*, 2004).

73 These traits, large panicle size and arrangement of the top three leaves they aim to increment the
74 sink size and the source of photoassimilates.

75 Photoassimilates are generated in the process namely photosynthesis which consists of the one
76 light phase and another dark phase. In the light phase, photons are trapped by pigments and
77 transport across the photosystem II (PSII) and I (PSI) in the called electron transport chain to
78 produce NADPH and ATP.

79 Rice is a C3 plant where photosynthesis is limited to use solar radiation because of the importance
80 of the photorespiration that enhancer the dissipation excess energy (Murchieet *al.*, 2015; Zhu et al.,
81 2010). Then, the control of the electron transport rate of the chain electron transport is a
82 fundamental concept in the regulation of photosynthesis (Foyer *et al.*, 2002).

83 Chlorophyll fluorescence is an important tool to investigate the behavior of the photosynthetic
84 capacity and potential, this technique is as a window inside to the heart of the photosynthetic
85 process (Stirbet and Govindjee 2011).

86 Different approaches have been realized to measure chlorophyll fluorescence, based on the
87 Kautsky effect. Among them is the called OJIP analysis, which is based on the fluorescence
88 transient of the PSII chlorophyll fluorescence and the terms concern to basal fluorescence level (F_0),
89 two intermediate steps namely J and I and a maximum fluorescence level ($F_p = F_m$) (Strasser *et al.*,
90 2000).

91 Basal fluorescence level F_0 indicated that all reaction center (RC) is open and it is assumed that at
92 F_m levels all RC is closed.

93 The J step occurs at 2ms from F_o and is related to reduction of the primary quinone electron
94 acceptor Q_A reduction, while I step occurs at the 20ms and is related to the Q_b reduction. Data
95 fluorescence is recorder as F_J and F_I , whilst data as fluorescence at $300\mu s$ and is used to calculate
96 the initial slope M_o that indicates the net ratio of RCs closure.

97 On another hand, the difference between F_o and F_m is called fluorescence variable (F_v) and the
98 ratio between F_v and F_m (F_v/F_m) is related to the maximum quantum yield of primary PSII
99 photochemistry, also expressed as the ratio JTR/JABS (Strasser *et al.*, 2000).

100 Other important parameters obtained from the OJIP analysis are the area over the curve namely
101 S_m that indicates a bulk of electron acceptors presented and the normalized S_m/F_v indicates the
102 energy need to close all RCs or the electron acceptors per active electron transport chain (Stirbet
103 and Govindjee 2011).

104 Other authors introduced a new parameter called performance index on energy absorbed (PI_{abs}).
105 This index is calculated with three components that included density of reaction center per energy
106 absorbed basis, energy trapping efficiency and the electron transport efficiency and can be defined
107 as a performance index for energy conservation from photons absorbed by PSII antenna, to the
108 reduction of Q_b (Srivastava *et al.*, 1999).

109 These and other parameters calculated of the OJIP analysis allow a deep examination of the
110 functionality of PSII and are an approach to understand the genetic variability intra/interspecies.

111 The genetic resources and chance to use this diversity depend on the ability to understanding the
112 genetic base of those traits.

113 Quantitative trait loci (QTL) were used extensively to explore the genetic basis of the important
114 agronomic trait. This QTL analysis developed through linkage mapping is a very time-consuming
115 approach due to the inbreeding line must be obtained and constructing by linkage mapping.
116 Moreover, the QTL acquired they come off the narrow genetic basis, hindering the use in the
117 breeding program.

118 In recent years, the new technique to obtained QTL and molecular markers for use in plant
119 breeding has been developed. This technique is based on the linkage disequilibrium and required a
120 high number of genotypes with a spread genetic basis (Yang *et al.*, 2018) and is called the genome-
121 wide association study (GWAS).

122 In rice, numerous populations were sequenced and used in studies of GWAS as the RDP1 and RDP
123 1+2 consisting of 421 y 1571 accessions respectively (McCouchet *et al.*, 2016), two populations
124 development in the National Center of Plant Gene Research with 533 and 950 accessions (Huang
125 *et al.*, 2012) and the 3243 rice accessions belonging to 3000 rice genome project (Li *et al.*, 2014).

126 The study of these sequenced populations allowed the development of the great number of GWAS
127 that covering diverse agronomic traits as heading date, plant height, grain length, spikelets for
128 panicle, etc. (Xie *et al.*, 2015; Crowell *et al.*, 2016; Spinde *et al.*, 2015; Begum *et al.*, 2015; Zhao *et al.*,
129 *et al.*, 2011; Biscarini *et al.*, 2016; Hu *et al.*, 2016; Han *et al.*, 2016), diverse biotic and abiotic stress (Li
130 *et al.*, 2017; Shakiba *et al.*, 2017; Kang *et al.*, 2016; Kumar *et al.*, 2015; Lafarge *et al.*, 2017; Shi *et al.*,
131 *et al.*, 2017; Kadam *et al.*, 2018; Pantalião *et al.*, 2016; Ma *et al.*, 2016) and diverse physiological traits
132 (Yang *et al.*, 2018; Yang *et al.*, 2018; Mogga *et al.*, 2018; Quero *et al.*, 2018).

133 Furthermore, currently, a great interest in describing rice phenotypes that may have better
134 efficiency in the electrons transport (Meacham *et al.*, 2017). In line with the above, there are
135 reports in rice that describe the relationship between PSII activity and grain yield (Wang *et al.*,
136 2014; Zhang *et al.*, 2015).

137 In the present study, we applied GWAS mapping to investigate the genetic architecture of PSII
138 efficiency under two environmental conditions and evaluated the interaction between the
139 behaviour of PSII and yield components. We analyzed PSII efficiency in RDP 1 population with
140 highly diverse rice genotypes; these populations were genotyped with 700,000 SNPs markers
141 (Crowell *et al.*, 2014). Indeed, these results are discussed in the context of the rice PSII efficiency
142 and they translated into yield.

143
144

145 **2. Material and methods.**

146

147 **2.1 GWAS germplasm selection.**

148 A collection of 283 accessions, belonging to the RDP-1 panel, representing the five major
149 subpopulations in *O. Sativa* genotyped to 700,000 SNPs (Crowell *et al.*, 2016) was used. The
150 accessions selected from the rice subpopulations were 45 *aus*, 59 *indica*, 58 *temperate japonica*,
151 76 *tropical japonica*, 8 *aromatics*, and 37 *admixed*.

152

153 **2.2 Experimental design and locations.**

154 The seeds were sown in Petri dishes on filter paper, rinsed with 7 mL carbendazim 0.025 %p/v, and
155 incubated at 30°C in darkness during three days until germination. The seedlings were cultured in a
156 growth chamber with 28/24 °C day/night temperatures, 12-12h photoperiod 240 $\mu\text{mol photons m}^{-2}$
157 s^{-1} of photosynthetically active radiation (PAR) and, 60% average humidity. The seedling was
158 growing in hydroponically conditions with nutritive Yoshida solutions (Yoshida *et al.*, 1976). After
159 two weeks germination seedling was transplanting to field conditions in pots containing mineral
160 soil. The accessions were planted in a randomized complete form with three replications.

161 Field experiments were conducted at two locations, INTECH, Chascomús- Buenos Aires (35.623048
162 -57.994167, CH), and EEA INTA Concepción del Uruguay, Entre Ríos (32.490254, -58.348855, ER).
163 Both experiments were performed in the summer season 2017/2018. The physiological
164 measurements were performed in plants of 11 old- weeks and all plants are in the tillering stage.

165

166 **2.3 Chlorophyll transient fluorescence measurements (OJIP test) and SPAD.**

167 Fluorescence transient was measured in the uppermost fully expanded leaf. Measurements were
168 taken with a plant efficiency analyzer (Handy PEA fluorometer, Hansatech Instruments Ltd., King's
169 Lynn, Norfolk, UK), according to the protocol used for the so-called double-hit experiments
170 (Appenroth *et al.*, 2001). Leaves were dark-adapted by 20 minutes using a leaf clip provided by the
171 manufacturer. Then, leaves were exposed twice for 1 s with 3000 $\mu\text{mol photons m}^{-2} \text{s}^{-1}$ (650 nm
172 peak wavelengths) with a dark interval of 0.5 seconds. In this line, the data become for the first hit
173 was extracted and used as a phenotypic fluorescence trait.

174 The fraction of Q_b reducing centers (Q_bRC) can be calculated as follows:

175

$$176 \quad Q_bRC = [1 - (F_0 / F_M)_{(2^{\circ} \text{ hit})} / 1 - (F_0 / F_M)_{(1^{\circ} \text{ hit})}] = \phi_{po}^* / \phi_{po}$$
$$177 \quad \text{Non- } Q_bRC = 1 - \phi_{po}^* / \phi_{po} = 1 - Q_bRC$$

178

179 The PEA plus software (PEA Plus software, Hansatech Instruments Ltd., UK) was used to analyze
180 the PSII parameters according to Strasser *et al.* (2000). The different OJIP parameters are present in
181 Table 1.

182 To estimate leaf total chlorophyll content, a SPAD chlorophyll meter was used (Cava-devices, CABA,
183 AR). For each leaf, the chlorophyll content was estimated as the mean of five chlorophyll content
184 measurements at different positions in the middle section of the leaf.

185

186 **2.4 Determination of yield components**

187 Plants were harvested at the maturation stage. The panicles were threshed manually and
188 processed by a hulling machine JLGJ-45 (JinGao, Cn) and the following yield components were
189 measured: the weight of one thousand grain (WTG), number of panicle per plant (PN), number of
190 spikelets per panicle (NSP), panicle weight (PW) calculated as the weight of filled grains per panicle,
191 percentage of fertile and infertile spikelets (%F and %In respectively). All dates are an average of
192 total panicles per plant replications.

193

194

195 **2.5 GWAS mapping.**

196 The GWA studies were performed based on the HDRA data set consisting of 700,000 SNPs
197 (McCouch *et al.*, 2016). Phenotypic grand means for each variety were used in the mapping models.
198 GWAS was performed using a linear mixed model with EMMAX algorithm (Kang *et al.*, 2010),
199 which takes the underlying population structure into account by including two kinship matrix (hBN
200 and hBS) as a covariate.

201 The maximum rates of missing data were fixed at 10% per accessions and 25% per SNP. A minor
202 allele frequency threshold of 0.05 (MAF<0.05) was applied to discard markers with very rare alleles
203 according to Aulchenko *et al.* (2007). The significance threshold was set at $p < 1.28 \times 10^{-7}$ for every
204 trait, using Bonferroni criteria.

205 **2.6 Linkage disequilibrium**

206 GWAS Linkage disequilibrium (LD) between markers on each chromosome was calculated using
207 pairwise r^2 between SNPs. First, we performed LD, calculated using the `--r2 --ld-window 99999 --`
208 `ld-window-r2 0` commands in PLINK (version 1.9) (Chang *et al.*, 2015).

209 The critical threshold used was 0.2 (McCouch *et al.*, 2016). Then, for each significant marker, we
210 computed LD upstream and downstream on the same chromosome as a mean LD value through
211 plotting r^2 1,000 SNPs of each chromosome versus genetic distance between markers we defined
212 both boundaries of the confident interval as the intersection of the 'critical LD' threshold and the
213 fitted curve of r^2 regression (See Supplementary. Fig.1). A nonlinear model described by
214 Remington *et al.* (2001) was used to fit the LD decay. The R function NLS (nonlinear least-squares
215 method) was used to fit the model. The number of genes within each interval was identified from
216 the rice genome.

217

218 **2.7 Statistical analyses.**

219 Histograms, boxplots, correlations and GWAS analyses were constructed using phenotypic grand
220 means for each variety. Manhattan plot and Qqplots (Suppl. Figure 2 and 3) were created using the
221 package `qqman()` in R (Rebolledo *et al.*, 2015). P -values for Pearson's correlation coefficients were
222 calculated with a two-sided t-test using the `cor.test()` function in R.

223 Analysis of variance was performed for genotype, environment, and genotype x environment using
224 the `lme4` function in R (Bates *et al.*, 2015).

225

226 **2.8 Gen candidate analysis**

227 A list of the candidate gene was constructed in the base to gen functional notation utilizing the
228 Rice Gene Annotation Project database ([http://rice.plantbiology.msu.edu/cgi-](http://rice.plantbiology.msu.edu/cgi-bin/batch_download.pl)
229 [bin/batch_download.pl](http://rice.plantbiology.msu.edu/cgi-bin/batch_download.pl)).

230 Also, an enrichment analysis of the GO terms (Gene Ontology) was performed, using the agriGO
231 analysis tool (<http://systemsbiology.cau.edu.cn/agriGOv2>; Du *et al.*, 2010). In this analysis, the list
232 of gen candidates derived from the GWAS mapping was used utilizing the Oryza Sativa LMSU
233 database with agriGO as a reference. The analysis was carried out using Fisher's statistical method
234 to detect significantly enriched ontological terms. The transcription factors (FT) identified were
235 classified according to the PlnTFDB web tool (the PlantTranscription Factor Database;
236 <http://plntfdb.bio.uni-potsdam.de/v3.0>; Pérez-Rodríguez *et al.*, 2009)

237

238 **3. Results**

239 **3.1 Phenotype and population structure.**

240 The rice diversity panel RDP-1 consists of 435 inbred accessions of *O. sativa* that come from 82
241 different countries (Zhao *et al.*, 2011). In this study, a part of the RDP-1 was cultivated under field
242 conditions in two different environmental locations, Chascomús (CH) and Entre Ríos (ER). Then,
243 283 plant accessions (from those above), were phenotyping at vegetative stage for photosynthetic
244 traits (PT) by measuring the fluorescence transient of chlorophyll a and the SPAD index. On the
245 other hand, a principal component analysis (PCA) was used to describe the overall genetic
246 variation in the RDP-1. The population presented a clear structuring of the accessions analyzed
247 caused by the environmental condition (Fig. 1). The top two principal components (PCs) explain
248 95.17% of the genetic variation within the panel (Figure 1). A total of 29 PT were measured for 283
249 accessions in RDP-1 at the vegetative stage and they were used for the GWAS analysis, in which all
250 rice subpopulations were represented: 45 aus, 59 indica, 58 temperate japonica, 76 tropical
251 japonica, 8 aromatic and 37 admixed. A brief description of the traits evaluated is summarized in
252 Table 1. In this sense, the analysis of variance (ANOVA) showed significant effects on the genetic
253 component (G), the environmental factor (E), and their interaction (GxE) (Table 1). However, some
254 exceptions were the RE_o/CS and $\delta(R_o)$ traits, that not showed significant E effects. In line with this
255 the P_Itotal not presented significant differences in G, E and GxE interaction (Table 1).

256

257

258

259 **3.2 Genome-wide association analysis.**

260 After filtering, the set of markers was constituted of 388,084 SNPs with MAF \geq 5%, within the
261 12 rice chromosomes. A total of 110 significant SNPs-trait associations were identified, intersecting
262 both sets of significant associations (obtained with hBS and hBN matrices, mention above).
263 Moreover, 11 of these significant SNP-trait associations corresponded to the cultivation plants in
264 CH environment, while 99 significant SNP-trait associations belonged to plants grown in the ER
265 environment (Table 2). Interestingly these associations being unique for each environment,
266 presenting none SNP in common between CH and ER. Likewise, of the total fluorescent
267 phenotypes evaluated here, 5 of them registered significant associations in both environments
268 with SNPs (F_o/F_m , F_v/F_m , DI_o/RC , $\delta(R_o)$, and PI_{abs} (Table 2) in both environments of the PT analyzed,
269 only the chlorophyll fluorescence phenotypes showed significant associations with SNPs. In line
270 with this, 6 significant fluorescent phenotype associations were detected in CH environment, while
271 in ER environment, a total of 13 phenotypes were significantly associated with some SNPs (Fig. 2A-
272 B; Table 2). The plants growing in the CH environment showed a lower mean value of the F_v/F_m and
273 PI_{abs} traits than ER environment, with differences of 7.23% and 57.27% respectively (Fig. 2).
274 However, other phenotypes like F_o/F_m , DI_o/RC , and $\delta(R_o)$ of the plants grown in CH showed higher
275 average values compared to the ER environment. These differences being 26.17% for the F_o/F_m ,
276 31.55% for the DI_o/RC , and 31.77% for the $\delta(R_o)$ (Fig. 2).

277 On the other hand, among the 110 SNPs mapped here for both environments, 70 SNPs were
278 associated with a single locus trait (Table 2). In this sense, others 11 associations found for CH, the
279 F_o/F_m , F_v/F_m , DI_o/RC , and DF_{abs} phenotypes mapped in the same SNP, SNP-5.11015630
280 (Supplementary Table S1), while the 6 associations found for the $\delta(R_o)$ phenotype were unique for
281 this parameter, as well as the only SNP identified for the PI_{abs} (Table 2).

282 Alternatively, in ER environment, 63 SNPs were associated with a single locus respectively
283 (Table 2), as for the CH environment, PI_{abs} phenotype mapped in a single significant SNP, SNP-
284 1.35479825 (Supplementary Table S1), while other 12 and 4 SNPs were associated together with
285 two and three fluorescence traits respectively (Supplementary Table S1). Among the 28
286 fluorescence traits analyzed here, the turnover of Q_a (N) and energy dissipated by active reaction
287 centers of FSII (DI_o/RC), were associated with the higher number of SNPs (24 SNPs, Table 2).

288 Likewise, a total of 69 QTLs were identified for 14 of 29 PT analyzed in both environments
289 tested and belonged to three classes. The first class of QTL was defined as single SNP associated
290 with a unique phenotype, the second class of QTL were those identified SNPs associated with more
291 than one phenotypes (multi-type QTL). Finally, the third class of QTL found corresponded to SNPs

292 mapped in chromosome region, where two or more SNPs separated by a distance of ~ 55 kb and
293 these were associated with a particular phenotype (QTL multi SNP). In line with this, the CH
294 environment, presented a single multi-type QTL on chromosome 5 (Fig. 3A), where a single SNP
295 was associated with the F_o/F_m , F_v/F_m , DI_o/RC , and DF_{abs} traits (SNP- 5.11015630).

296 On the other hand, for the ER environment, 4 multi-type QTLs were identified on
297 chromosomes 2, 3, 4, and 6 (Fig. 4A), where the RE_o/RC , N, and Sm phenotypes shared the SNP
298 SNP-2.18755532 (Supplementary Table S1). At the same time, the $\delta(R_o)$, DI_o/CS , and DI_o/RC
299 phenotypes shared the SNP, SNP-3.7631091. In turn, the DI_o/RC phenotypes shared SNP-
300 4.3532129 with the N and RE_o/RC phenotypes. Finally, the F_o/F_m , F_v/F_m , and $\delta(R_o)$ traits were
301 jointly associated with the locus SNP-6.21617771 (Fig. 4A; Supplementary Table S1).

302 Besides, another 4 QTL multi-types were identified for S_m and N on chromosomes 1, 4, 5, and
303 10 (SNPs 1.32181171, 4.19830956, 5.13606968 and 10.2073752). In addition one more multi-type
304 QTL of interest was found for the energy dissipation phenotypes DI_o/RC and DI_o/CS , on
305 chromosome 11; SNP11.9898109 (Fig. 4A). Finally, 5 QTL multi SNPs were detected, 3 of these
306 were associated with DI_o/RC trait on chromosomes 1, 3, and 5 (Fig. 4A), and other one for the
307 Q_bRC onto chromosomes 12 (Fig. 4B). The remaining 59 QTLs identified corresponded to the single
308 SNP class (Fig. 4A-B).

309

310 **3.3 Identification of candidate genes.**

311 The genome browser feature of Rice base "Rice Annotation Project"
312 <http://rice.plantbiology.msu.edu/index.shtml>, was used to identify candidate genes based on the
313 MSU7 gene annotation. The selection of candidate genes was underlined for each QTL accordingly
314 the linkage disequilibrium (LD) (Supplementary Table S2). These genes were classified accordingly
315 their Gene ontology (GO) term. Subsequently the enrichment analysis of the list of total candidate
316 genes showed a significant proportion of genes involved on molecular functions related to cell
317 biosynthesis (GO: 0044249), metabolic regulation processes (GO: 0019222), regulation of gene
318 expression and macromolecular processes (GO: 0010468, GO: 0060255), processes related to cell
319 death (GO: 0008219), macromolecule cell biosynthesis (GO: 0034645), and macromolecule
320 biosynthesis (GO: 0009059) also showed significant enrichment (Table 3). Furthermore the most
321 represented terms linked to biological processes were related to hydrolysis processes of acids,
322 phosphate and ester groups (GO: 0016817, GO: 0017111, GO: 0016818, GO: 0016462 and GO:
323 0016788) and nucleotide-binding (GO: 0000166).

324 Based on these most representative GO terms, 38 candidate genes were highlighted in Table 4
325 from the 157 total candidate genes mapped (Supplementary Table S2).

326 Of those 38 candidate genes 8 genes corresponded to genes associated with response to biotic
327 and abiotic stress (LOC_Os01g02250, LOC_Os03g59600, LOC_Os05g44340, LOC_Os06g30430,
328 LOC_Os08g28470, LOC_Os09g26620, LOC_Os12g03750, and LOC_Os12g30150). Also, 5 genes
329 were identified as transcription factors (LOC_Os03g17130, LOC_Os03g20900, LOC_Os05g23780,
330 LOC_Os05g44400 and LOC_Os10g39030), one gene was assigned to the Calvin Cycle
331 (LOC_Os05g44922). Likewise, three identified genes are linked to functions associated with grain
332 characters (LOC_Os05g02670, LOC_Os05g44560, and LOC_Os10g39030); and finally, a gene with
333 functional notation linked to senescence processes (LOC_Os05g44970). Based on these results, it
334 could be said that the genetic architecture of the functionality of the PSII can be associated at the
335 genetic level mainly with processes linked to grain filling among other processes.

336

337 **3.4 Relationships between panicle traits and FSII parameters.**

338 Six panicle traits were evaluated: Number of Panicle per Plant (PN), Thousand Grain Weight (WTG),
339 Fertility Percentage (%F), Calculated Infertility Percentage (%In), Number of Spikelet per Panicle
340 (NSP) and Panicle Weight (PW).

341 These panicle traits showed different distribution depending on the environmental condition.
342 Plants grown in the environmental conditions of ER showed higher NP, NSP, %In, and PW compared
343 with plants grown in the CH; these differences were 15.1%, 45.6%, 26.1%, and 27.4% respectively
344 (Fig. 5). Meanwhile, the WTG and %F traits were 10.3% and 19.80% lower for the ER environment
345 compared to the CH environment (Figure 5).

346 The analyses of Pearson's correlation coefficients were calculated between all the FSII parameters
347 associated with the identified candidate genes (Supplementary Table S3) and panicle traits in both
348 environmental conditions (CH and ER) allowed identifying some significant relationships. The top
349 ranking significantly were: one negative correlation between and a positive correlation with the
350 $\delta(R_o)$ phenotype in CH condition. Sequentially, the $\delta(R_o)$ phenotype also showed a positive
351 correlation with the NSP panicle trait (Supplementary Table S3).

352 On the other hand, the correlation analyses between, panicle traits and FSII parameters for the ER
353 environment were in general significant among themselves. In line with this, the mean of r
354 Pearsoncoefficient between pairs of fluorescence phenotypes and panicle traits, which were
355 statistically significant was $r = 0.14$. For this reason, the correlations that presented an $r > 0.14$ were
356 analyzed (Supplementary Table S3).

357 From the correlation diagram (Supplementary Table S3), it can be seen that the %In trait correlates
358 positively with the N and DI_o/RC phenotypes. Also, the NSP trait correlated positively with the
359 RE_o/RC phenotype, correlated negatively with the PI_{total} phenotype. On the other hand, the PW
360 panicle trait presented 4 significant correlations with fluorescence phenotypes, which is the trait
361 that presented the greatest amount of correlations. The four significant correlations, three were
362 negative with the N, DI_o/RC , and PI_{total} phenotypes, while the remaining correlation was positive
363 with the RE_o/RC phenotype.

364 On the other hand, the WTG and %F traits correlated significantly with the same fluorescence, N,
365 and DI_o/RC phenotypes; being in both cases negative correlations. Finally, the PN panicle trait only
366 correlated significantly and negatively with the PI_{total} fluorescence phenotype.

367

368 **4. Discussion**

369

370 Mapping genetic regions that control quantitative features of PSII functionality is a difficult task
371 because photosynthetic processes have a complex and polygenic architecture. Our results showed
372 a clear effect of the environment on the population genetic structure evidenced by the segregation
373 into two groups of different individuals represented by plants grown in the CH and ER
374 environments (Fig. 1).

375 In plants, chlorophyll fluorescence has been used extensively to examine the influence of abiotic
376 stresses on light-dependent reactions (Fracheboud *et al.*, 1999; Huang *et al.*, 2004; Silvestre *et al.*,
377 2014; Rachoski *et al.*, 2015). However, despite the versatility of the use of chlorophyll fluorescence
378 as a rapid phenotyping method, and of great capacity to evaluate numerous plant accessions, few
379 reports study the mapping of regions or the genetic variation of fluorescence phenotypes in
380 environmental conditions. Nonetheless, QTL for photosynthetic phenotypes associated with light
381 reactions has been successfully mapped in some species of agronomic importance such as wheat,
382 corn, soybeans, and sorghum (Šimić *et al.*, 2014; Herritt *et al.*, 2016; Ortiz *et al.*, 2017).

383 The reactive processes of the PSII are sensitive to light, and in turn, the light that impacts the PSII
384 depends strongly on the environmental conditions. The natural variations are an important
385 approach to identify new genetic determinants to improve the efficiency of the use of crop light.
386 Since the phenotypic variation of the functionality of the photosynthetic apparatus (PA) of the
387 RDP-1 was measured under normal non-stressful conditions in two environmental locations and
388 the environmental impact on the genetic architecture of the PA could be assessed. Our results
389 showed that fluorescence phenotypes evaluated are highly influenced by genotype, environmental
390 conditions, and genotype-environment interaction (Table 1). Similar results were found in studies

391 in soybean, where chlorophyll fluorescence phenotypes were analyzed in various environments
392 (Herritt *et al.*, 2016). On the other hand, in rice, the analysis of other photosynthetic parameters
393 such as stomatal conductance (G_s), net photosynthesis (A_{sat}), and photochemical performance
394 F_v/F_m were affected by environmental, genotypic factors and their interaction between them (Qu
395 *et al.*, 2017). In other words, our results show that the significant natural variation in each
396 chlorophyll fluorescence phenotype observed among a plethora of rice genotypes indicates that
397 the selection of these photosynthetic features as an improvement criterion could be possible.

398 In this sense, of the significant phenotypes found in both environments F_o/F_m , F_v/F_m , DI_o/RC , PI_{abs}
399 and $\delta(R_o)$, it was observed that the average values obtained for the ER environment were higher
400 compared to the Ch (Fig. 2A-B). In this line, the F_o/F_m phenotype is the basis of all the expressions
401 derived from the OJIP test. This phenotype allows the phenomenological quantification of the
402 fluorescence behavior of a sample, and at the same time, compares and classifies different types
403 of samples (Strasser *et al.*, 2000). The phenotype F_v/F_m is used to quantify the physiological state
404 of plants (Baldassarre *et al.*, 2011). The phenotype PI_{abs} indicates the status of FSII, from the
405 absorption of a photon by FSII to the reduction of Q_b (Stirbet and Govindjee 2011). Finally, the
406 DI_o/RC and $\delta(R_o)$ phenotypes explain the energy dissipation by active reaction center and the
407 efficiency of electron transport to the last FSI acceptor respectively (Stirbet *et al.*, 2018).

408 GWAS studies using chlorophyll fluorescence under optimal stress and growth conditions have
409 been reported in soybeans, corn, and sorghum (Hao *et al.*, 2012; Strigens *et al.*, 2013; Fiedler *et al.*,
410 2016). In all cases, the photosynthetic phenotype features were associated with multiple regions
411 within the genome. Results of the present work yielded 110 QTL in all chromosomes and even the
412 same phenotype was associated in more than one region within the same chromosome according
413 to those previous reports (Fig. 3A; 4A-B). Particularly for the CH environment, a QTL was identified
414 on chromosome 9 for the PI_{abs} phenotype, this phenotype has a unique association on the said
415 chromosome, and in turn, this was the unique association found on this chromosome (Fig. 3B).
416 This fact makes the PI_{abs} phenotype an interesting study target in plant improvement projects since
417 this type of association is an exception to the results conventionally found in GWAS studies for
418 chlorophyll fluorescence phenotypes.

419 In addition to the difference in the number of SNPs and the phenotypic variation observed
420 between the environments, and as consequence a greater number of QTL for the ER environment
421 were also identified. In line with those mentioned, GWAS studies in *Arabidopsis thaliana* YELLOW
422 SEEDLING G1 (YS1) revealed diversity in photosynthetic acclimatization under high radiation

423 conditions, finding a greater amount of QTL than in low radiation conditions (van Rooijen *et al.*,
424 2017).

425 The analysis of the QTL for the CH environment yielded a single multi-type QTL on chromosome 5
426 (Fig. 3), unlike the ER environment where 4 multi-type QTLs could be identified (Fig. 4). In both
427 environments, the F_o/F_m , F_v/F_m , and DI_o/RC phenotypes share the same QTL on chromosome 5 for
428 plants in CH and chromosome 6 in the ER plants. Identical results were obtained in studies
429 conducted in soybeans (Herritt *et al.*, 2016); where the phenotypes of the relationship between
430 maximum and minimum fluorescence, the maximum quantum yield of PSII, and energy dissipation
431 per active reaction center share the same region within the chromosome.

432 The regions of the genome found by molecular markers for fluorescence phenotypes contained
433 groups of genes that are important for the metabolic and molecular functioning of rice.
434 Additionally, these regions encompassed individual genes that have a significant impact on the
435 functions of grain filling, and therefore, the values of some chlorophyll fluorescence phenotypes
436 could directly influence the grain yield of rice. The examination of the genetic annotations linked to
437 the enrichment analysis of GO terms identified in this study revealed 38 candidate genes (Table 4).
438 Of the identified candidate genes, those with catalytic activity notations formed the majority group
439 (Tables 3 and 4).

440 When analyzing how fluorescence phenotypes are related to the identified genes, it was observed
441 that the S_m and N phenotypes, in general, are associated with the same identified genes (Table 4).
442 Phenotype N indicates the number of reduction and oxidation events of Q_a between time zero and
443 F_m (Strasser *et al.*, 2000). In turn, the S_m phenotype indicates the energy required for electron
444 transport, and thus, closes all reaction centers (Oukarroum and Strasser 2004), this is equivalent to
445 saying that S_m indicates the functionality of the quinone complexes (Q_a/Q_b). Both phenotypes are
446 highly related to the functioning of the set of quinones, therefore, this may explain that both
447 phenotypes are linked to the same genes. In this sense, of the 5 transcription factors (TF) identified
448 two of them co-located with both phenotypes N and S_m (LOC_Os10g39030, LOC_Os05g23780). The
449 functional notation assigned for the first TF corresponded to the homeobox (HD) domain, while a
450 second TF codes for the OsMADS70-MADS-box family of genes with M-alpha type-box (MADS-
451 BOX). Others GWAS reports for panicle traits in RDP-1 populations mapped genes containing both
452 types of HD and MADS-BOX domains associated with flowering time, and the plant height (Begum
453 *et al.*, 2015).

454 The HD domain is a highly conserved motive present in many TFs. At the same time, work carried
455 out with mutant rice plants for HD domains in different TFs showed that those HD domains are

456 essential for the regulation of tillering, sterility and flowering time in rice (Mjomba *et al.*, 2016;
457 Wei *et al.*, 2016). On the other hand, in rice, the FT MADS-BOX besides being involved in the
458 specification of the floral organs has also been involved in several aspects of the growth and
459 development of the plants (Arora *et al.*, 2007). In this sense, Lee *et al.* (2004) showed that mutants
460 of the MADS-BOX family of rice presented a delay in flowering, while in rice plants that
461 overexpressed genes of the MADS-BOX family, extremely early flowering was observed.

462 Of the remaining three TFs, one is associated with the Q_bRC phenotype (β Helix-loop-helix) and two
463 identified TFs were associated with DI_o/RC (GATA zinc finger domain and Myb). In all cases, these
464 TFs were associated with different types of abiotic stress. Besides, DI_o/RC is also linked to TF HD by
465 co-locating with the N and S_m phenotypes. Likewise, the DI_o/RC phenotype presented a large
466 number of identified genes, mainly in plants that were grown in the ER environment. In general,
467 the genes identified were associated only with the DI_o/RC phenotype. In this sense, the energy
468 dissipation processes have been described as a fundamental mechanism in the photo protection of
469 plants, in response to the excess of light that affects the complex antenna of the chloroplast
470 (Müller *et al.*, 2001).

471 Among the identified candidate genes associated with the DI_o/RC, the LOC_Os05g44922 and
472 LOC_Os05g44560 genes can be highlighted. For the first of these two genes, the assigned
473 functional notation corresponded to 6-phosphofructokinase (PFK), an intermediate enzyme in the
474 glycolysis pathway conducted by the Calvin cycle. It has been described that PFK is a key
475 intermediary in the synthesis of the main starch component of rice grain (Chang *et al.*, 2017). For
476 the second candidate gene, the functional notation corresponded to the genes of the Kinesin
477 family.

478 In rice, kinesins are linked to cell division processes and are expressed in both pollen grains and
479 somatic tissues. In turn, studies conducted on rice indicated that genes from the kinesin family
480 regulate plant height and seed length (Zhang *et al.*, 2010; Kitagawa *et al.*, 2010).

481 Finally, of the two most representative phenotypes evaluated in CH environment, δ (R_o) was
482 associated with a gene that contained the kinesin motor domain, a similar result was identified for
483 DI_o/RC phenotype. Furthermore, the PI_{abs} phenotype underlying with LOC_Os09g26620 *loci* that
484 codes for an auxin-repressed protein. Previous reports showed this gene family regulated tillering
485 (Zhang *et al.*, 2018). In line with the aforementioned, it has been reported that a large number of
486 tillers limit the remobilization of resources generated by photosynthesis to the final destination,
487 the grain, limiting the yield potential, and increasing biomass (Khush, 1995).

488 The analysis of panicle traits showed a greater accumulation of positive characters such as PN, NSP,
489 and PW in plants grown in the ER, compared with plants grown in CH (Fig.5). However, even
490 though the plants grown in the ER showed a greater number of destinations in their panicle
491 features, they presented a higher %In (Fig. 5). The higher %In could be that for the ER
492 environment the variability of genotypes that managed to reach the reproductive stage was more
493 diverse within the sub-populations of the RDP-1.

494 From the correlation diagram for CH (Supplementary Table S3), it was observed that the PI_{abs}
495 phenotype correlated negatively with the NP trait or what is equivalent to saying that when PI_{abs}
496 increase there are fewer panicles per plant. This result coincides with the lower value of NP found
497 in CH plants compared to plants grown in ER (Fig. 5) and with the function described for the
498 identified gene linked to this phenotype. In concordance it has been reported that a greater
499 tendency of plants to increase their tillering allocates photosynthetic resources to generate
500 biomass at the expense of limiting resources destined to the panicle (Khush, 1995). Concerning the
501 $\delta(R_o)$ phenotype, this correlated negatively with NSP and positively with NP. Again, these results
502 are consistent with the underlying gene identified for this phenotype, the kinesins, whose main
503 function is cell proliferation since a higher value of $\delta(R_o)$ has a higher PN, although a lower NSP.

504 Alternatively in the ER location, the N parameter evaluated, negatively correlated with the panicle,
505 PW, WTG, and % F characters, positively with the %In trait, in turn, RE_o/RC positively correlated
506 with NSP and PW (Supplementary Table S3), indicating that a lower number of reduction and
507 oxidation cycles of Q_a and greater electron transport favors panicle performance. Finally, the
508 DI_o/RC phenotype showed the same correlations as for the N phenotype. These phenotypes were
509 linked to genes described as essential for grain yield. Energy dissipation has been described as a
510 photo protection mechanism to optimize photosynthetic efficiency at the canopy level achieving
511 an increase in biomass and yield in rice (Murchie *et al.*, 2015).

512 In conclusion, this work contributed with the identification of genetics determinants of chlorophyll
513 fluorescence diversity in rice by GWAS at two contrasting conditions and how these FSII
514 parameters are related with panicle characteristics. Manifold genes, SNP, and QTL identified here
515 may serve for the design of molecular markers and contribute to the assistance of breeding
516 programs of this species.

517 The improvement of the photosynthesis capacity in rice constitutes a goal to increased field yields
518 and this work could contribute to it.

519
520
521

522 **Supplementary data:**

523

524 **Supplementary Figure 1:** Graph of LD vs Genetic distance. The figure shows the graphic analysis of
525 chromosomes 1 to 12.

526 **Supplementary Figure 2:** Quantile-Quantile graph (QQplot) for the CH environment. The figure
527 shows the phenotype with significant associations.

528 **Supplementary Figure 3:** Quantile-Quantile graph (QQ plot) for the ER environment. The figure
529 shows the phenotype with significant associations.

530

531 **Supplementary Table 1:** Significant associated SNPs markers to PSII identified by GWAS analysis.
532 SNPs linked to their respective fluorescence phenotype, environment and matrix structure are
533 shown.

534 **Supplementary Table 2:** Total candidate genes identified by GWAS analysis in CH and ER
535 environments.

536 **Supplementary Table 3:** Correlation diagram between Panicle traits and PSII fluorescence
537 phenotypes for the Ch and ER environment. Asterisks indicate significant correlation according to
538 the Pearson pairwise correlation method (* $p < 0.05$).

539

540 **Data availability statement:**

541 All data supporting the findings of this study are available within the paper and within its
542 supplementary materials published online.

543

544

545 **Acknowledgments:**

546 This work was supported by grant StartUp 2013 0399 provided by Agencia Nacional de Promoción
547 Científica y Técnica (ANPCyT). This work is part of the PhD thesis of JMV.

548

549

550 **Author contribution**

551

552 JMV, EB, MLP, AAR, and SJM: investigation

553 JMV, EB, and SJM: formal analysis, writing.

554 AAR: funding acquisition

555 AL, JC, and OAR: resources

556 FC: validation

557 SJM: conceptualization

558

559

560

561

562

563

564

565

566

567

568

569

570

References:

Appenroth K, Sto J. 2001. Multiple Effect of Chromate on the Photosynthetic Apparatus of SpirodelaPolyrhiza as Probed by OJIP Chlorophyll a Fluorescence Measurements. Environmental Pollution 115 (1),49-64.

Arora R, Agarwal P, Ray S, Singh A, Singh V, Tyagi A, Kapoor S. 2007. MADS-Box Gene Family in Rice: Genome-Wide Identification, Organization and Expression Profiling during Reproductive Development and Stress. BMC Genomics 8, 242-253.

Aulchenko YS, Ripke S, Isaacs A, van Duijn CM. 2007.GenABEL: An R library for genome-wide association analysis. Bioinformatics23:1294–1296.

Baldassarre V, Cabassi G, Ferrante A. 2011. Use of Chlorophyll a Fluorescence for Evaluating the Quality of Leafy Vegetables. Australian Journal of Crop Science 5 (6), 735–741.

Bates Det al. 2015. Fitting linearmixed-effects models using lme4. Journal of Statistical Software, 67(1), 1–48.

Begum H, Spindel J, Lalusin A, Borromeo T, Gregorio G, Hernandez J, Virk P, Collard B, McCouch SR. 2015. Genome-wide association mapping for yield and other agronomic traits in an elite breeding population of tropical rice (*Oryza sativa*) PLoS ONE 10 doi: 10.1371/journal.pone.0119873.

Biscarini F, Cozzi P, Casella L, Riccardi P, Vattari A, Orasen G, Perrini R, Tacconi G, et al. 2016. Genome-Wide association study for traits related to plant and grain morphology, and root architecture in temperate rice accession. PLOS One doi: 10.1371/journal.pone.0155425

Chang CC, Chow CC, Tellier LCAM, Vattikuti S, Purcell SM, Lee JJ. 2015. Second-generation PLINK: rising to the challenge of larger and richer datasets.Gigascience 25;4:7. doi: 10.1186/s13742-015-0047-8.

Chang T, Liu C, Lin Y, Li C, Wang A, Chien M, Wang C, Lai C. 2017. Mapping and Comparative Proteomic Analysis of the Starch Biosynthetic Pathway in Rice by 2D PAGE/MS. Plant Molecular Biology 95 (4–5) 333–343.

Crowell S, FalcaoA, Shah A, Wilson Z, Greenberg A, McCouch S. 2014. High-Resolution Inflorescence Phenotyping Using a Novel Image-Analysis Pipeline, PANorama. Plant Physiology 165 (2): 479–95. <https://doi.org/10.1104/pp.114.238626>.

Crowell S, Korniliev P, Falcão A, Ismail A, Gregorio G, Mezey J, McCouch. 2016. Genome-wide association and high-resolution phenotyping link *Oryza sativa* panicle traits to numerous trait-specific QTL clusters. *Nature Communications* doi :10.1038/ncomms10527.

FAO.2009. Increasing Crop Production Sustainably. The Perspective of Biological Processes (Food and Agriculture Organization of the United Nations, Rome.

Fiedler K, Bekele W, Matschegewski C, Snowdon R, Wieckhorst S, Zacharias A, Uptmoor R. 2016. Cold Tolerance during Juvenile Development in Sorghum: A Comparative Analysis by Genomewide Association and Linkage Mapping. *Plant Breeding* 135 (5), 598–606.

Foyer C, Vanacker H, Gomez L, Harbinson J. 2002. Regulation of Photosynthesis and Antioxidant Metabolism in Maize Leaves at Optimal and Chilling Temperatures: Review. *Plant Physiology and Biochemistry* 40 (6–8), 659–68.

Fracheboud Y, Haldimann P, Leipner J, Stamp O. 1999. Chlorophyll Fluorescence as a Selection Tool for Cold Tolerance of Photosynthesis in Maize (*Zea Mays* L.). *Journal of Experimental Botany* 50 (338), 1533–1540.

Garris, Amanda J, Tai T, Coburn J, Kresovich S, McCouch S. 2005. Genetic Structure and Diversity in *Oryza Sativa* L. *Genetics* doi: org/10.1534/genetics.104.035642.

Hao D, Chao M, Yin Z, Yu D. 2012. Genome-Wide Association Analysis Detecting Significant Single Nucleotide Polymorphisms for Chlorophyll and Chlorophyll Fluorescence Parameters in Soybean (*Glycine Max*) Landraces. *Euphytica* 186 (3), 919–31.

Han Z, Zhang B, Zhao H, et al. 2016. Genome-wide association studies reveal that diverse heading date genes respond to short and long daylengths between indica and japonica rice. *Frontier in Plant Science* doi:10.3389/fpls.2016.01270.

Herritt M, Dhanapal A, Fritschi F. 2016. Identification of Genomic Loci Associated with the Photochemical Reflectance Index by Genome-Wide Association Study in Soybean. *The Plant Genome* 9 (2):1-12.

Hu Y, Huang Y, Zhang L, et al. 2016. Genome-wide association analysis reveals flowering? related genes regulating rachis length in rice. *Plant Breeding* 135(6), 677-682.

Huang Z, Jiang D, Yang Y, Sun J, Jin S. 2004. Effects of Nitrogen Deficiency on Gas Exchange, Chlorophyll Fluorescence, and Antioxidant Enzymes in Leaves of Rice Plants. *Photosynthetica* 42 (3), 357–364.

Huang X, Zhao Y, Wei X, Li C, Wang A, Zhao Q, Li W, Guo Y, et al. 2012. Genome-wide association study of flowering time and grain yield traits in a worldwide collection of rice germplasm. *Nature* 44,32-39.

Kadam N, Struik P, Rebolledo M, Yin X, Jagadich K. 2018. Genome-wide association reveals novel genomic loci controlling rice grain yield and its component traits under water-deficit stress during the reproductive stage. *Journal of Experimental Botany* 69 (16), 4017–4032.

Kang H, Wang Y, Peng S, et al. 2016. Dissection of the genetic architecture of rice resistance to the blast fungus *Magnaportheorizae*. *Molecular Plant Pathology* doi: 10.1111/mpp.12340

Kang HM, Sul JH, Service SK, Zaitlen NA, Kong SY, Freimer NB, Sabatti C, Eskin E. 2010. Variance component model to account for sample structure in genome-wide association studies. *Nature Genetics* doi: 10.1038/ng.548

Kumar V, Singh A, Mithra S, et al. 2015. Genome-wide association mapping of salinity tolerance in rice (*Oryza sativa*). *DNA Res.* 22 (2), 133–145.

Khush G. 1995. Breaking the Yield Barrier of Rice. *Geo. J.* Vol. 35.

Lafarge T, Bueno C, Frouin J, Jacquin L, Courtois B, Ahmadi N. 2017. Genome-wide association analysis for heat tolerance at flowering detected a large set of genes involved in adaptation to thermal and other stresses. *PLoS One* doi:10.1371/journal.pone.0171254.

Lee S, Kim J, Han J, Han M, An G. 2004. Functional Analyses of the Flowering Time Gene *OsMADS50*, the Putative Suppressor of Overexpression of *CO 1/Agamous-Like 20 (SOC1/AGL20)* Ortholog in Rice. *Plant Journal* 38 (5), 754–764.

Li J, Wang J, Zeigler R. 2014. The 3000 genomes project: new opportunities and challenges for future rice research. *GigaScience* 3, 8.

Li X, Guo Z, Lv Y, et al. 2017. Genetic control of the root system in rice under normal and drought stress conditions by genome-wide association study. *PLOS Genetics*, doi:10.1371/journal.pgen.1006889.

Ma X, Feng F, Wei H, et al. 2016. Genome-wide association study for plant height and grain yield in rice under contrasting moisture regimes. *Frontiers in Plant Science* doi:10.3389/fpls.2016.01801

McCouch S, Wright M, Tung C, Maron L, McNally K, Fitzgerald M, Singh N, et al. 2016. Open Access Resources for Genome-Wide Association Mapping in Rice. *Nature Communications* doi: org/10.1038/ncomms10532.

Meacham K, Sirault X, Quick P, Susanne von Caemmerer, and Robert Furbank. 2017. Diurnal Solar Energy Conversion and Photoprotection in Rice Canopies. *Plant Physiology* 173 (1), 495–508.

Mjomba FM, Zheng Y, Liu H, Tang W, Hong Z, Wang F, Wu W. 2016. Homeobox Is Pivotal for *OsWUS* Controlling Tiller Development and Female Fertility in Rice. *G3* 6 (7), 2013-2021.

Mogga M, Sibiya J, Shimelis H, Lamo J, Yao N. 2018. Diversity analysis and genome-wide association studies of grain shape and eating quality traits in rice (*Oryza sativa* L.) using DArT markers. PLoS ONE doi:10.1371/journal.pone.0198012.

Murchie, E, Ali A, Herman T. 2015. Photoprotection as a Trait for Rice Yield Improvement: Status and Prospects. *Rice* 8 (1), 31.

Müller P, Li X, Niyogi K. 2001. Non-Photochemical Quenching. A Response to Excess Light Energy. *Plant Physiology* 125 (4), 1558–1566.

Ortiz D, Hu J, Salas Fernandez M. 2017. Genetic Architecture of Photosynthesis in Sorghum Bicolor under Non-Stress and Cold Stress Conditions. *Journal of Experimental Botany* 68 (16), 4545–4557.

Oukarroum A, Strasser R. 2004. Phenotyping of Dark and Light Adapted Barley Plants by the Fast Chlorophyll a Fluorescence Rise OJIP. *South African Journal of Botany* 70 (2), 277–283.

Pantalião G, Narciso M, Guimarães C, et al. 2016. Genome wide association study (GWAS) for grain yield in rice cultivated under water deficit. *Genetica* 144, 651–664.

Peng S, Ismail A. 2004. Physiological basis of yield and environmental adaptation in rice. In: Nguyen HT, Blum A, eds. *Physiology and biochemistry integration for plant breeding*. New York: Marcel Dekker, 83–140.

Purcell S, Neale B, Todd-Brown K, Thomas L, Ferreira M, Bender D, Maller J, et al. 2007. PLINK: A Tool Set for Whole-Genome Association and Population-Based Linkage Analyses. *American Journal of Human Genetics* doi: org/10.1086/519795.

Qu M, et al. 2017. Leaf Photosynthetic Parameters Related to Biomass Accumulation in a Global Rice Diversity Survey. *Plant Physiology* 175 (1), 248–258.

Quero R, Gutiérrez E, Monteverde P, et al. 2018. Genome-wide association study using historical breeding populations discovers genomic regions involved in high-quality rice. *Plant Genome* doi: 10.3835/plantgenome2017.08.0076.

Rachoski M, Gazquez G, Calzadilla P, Bezus R, Rodriguez A, Ruiz O, Menendez A, Maiale S. 2015. Chlorophyll Fluorescence and Lipid Peroxidation Changes in Rice Somaclonal Lines Subjected to Salt Stress. *Acta Physiologiae Plantarum* 37, 117.

van Rooijen R, Kruijer W, Boesten R, van Eeuwijk FA, Harbinson J, Aarts MGM. 2017. Natural variation of YELLOW SEEDLING1 affects photosynthetic acclimation of *Arabidopsis thaliana*. *Nature Communications* 8: 1421.

Rebolledo MC et al. 2015. Phenotypic and genetic dissection of component traits for early vigour in rice using plant growth modelling, sugar content analyses and association mapping. *J Exp Bot* 66(18):5555

Remington D et al. 2001. Structure of linkage disequilibrium and phenotypic associations in the maize genome. *PNAS* 98 (20), 11479-11484.

Sasaki T. 2005. The map-based sequence of the rice genome. *Nature* 436: 793-800.

Šimić D, Lepeduš H, Jurković V, Antunović J, Cesar V. 2014. Quantitative Genetic Analysis of Chlorophyll a Fluorescence Parameters in Maize in the Field Environments. *Journal of Integrative Plant Biology* 56 (7): 695–708.

Shakiba E, Edwards J, Jodari F, Duke S, Baldo A, Korniliev P, McCouch S, Eizenga G. 2017. Genetic architecture of cold tolerance in rice *Oryza sativa* determined through high-resolution genome-wide analysis. *PLOS one* doi:12:3 10.1371/journal.pone.0172133.

Shi Y, Gao L, Wu Z, Zhang X, Wang M, Zhang C, Zhang F, Zhou Y, Li Z. 2017. Genome-wide association study of salt tolerance at the seed germination stage in rice. *BMC Plant Biology* doi:10.1186/s12870-017-1044-0.

Silvestre S, de Sousa Araújo S, VazPatto M, Marques da Silva G. 2014. Performance Index: An Expedient Tool to Screen for Improved Drought Resistance in the Lathyrus Genus. *Journal of Integrative Plant Biology* 56 (7), 610–621.

Spindel J, Begum H, Akdemir D, Virk P, Collard B, Redona E, Atlin G, Jannink JL, McCouch S. 2015. Genomic selection and association mapping in rice (*Oryza sativa*): effect of trait genetic architecture, training population composition, marker number, and statistical model on accuracy of rice genomic selection in elite, tropical rice breeding lines. *PLOS Genetics* doi: 10.1371/journal.pgen.1004982.

Srivastava A, Strasser R, Govindjee. 1999. Greening of peas: parallel measurements on 77k emission spectra, OJIP chlorophyll a fluorescence transient, period four oscillation of the initial fluorescence level, delayed light emission, and P700. *Photosynthetica* 37, 365–392.

Stirbet A, Govindjee. 2011. On the Relation between the Kautsky Effect (Chlorophyll a Fluorescence Induction) and Photosystem II: Basics and Applications of the OJIP Fluorescence Transient. *Journal of Photochemistry and Photobiology B: Biology* 104 (1–2), 236–57.

Stirbet A, Lazár D, Kromdijk J, Govindjee. 2018. Chlorophyll a Fluorescence Induction: Can Just a One-Second Measurement Be Used to Quantify Abiotic Stress Responses?. *Photosynthetica* 56 (1), 86–104.

Strasser R, Srivastava A, Tsimilli-Michael M. 2000. The Fluorescence Transient as a Tool to Characterize and Screen Photosynthetic Samples. In: Yunus M, Pathre U, Mohanty P, eds. Probing Photosynthesis: Mechanism, Regulation & Adaptation, CRC Press, 445–83.

Strigens A, Freitag N, Gilbert X, Grieder C, Riedelsheimer C, Schrag T, Messmer R, Melchinger A. 2013. Association Mapping for Chilling Tolerance in Elite Flint and Dent Maize Inbred Lines Evaluated in Growth Chamber and Field Experiments. *Plant, Cell, and Environment* 36 (10), 1871–1887.

Wang Y, Zhang J, Yu J, Jiang X, Sun L, Wu M, Chen G, and Chuangen L. 2014. Photosynthetic Changes of Flag Leaves during Senescence Stage in Super High-Yield Hybrid Rice LYPJ Grown in Field Condition. *Plant Physiology and Biochemistry* 82, 194–201.

Wei J, Choi H, Jin P, Wu Y, Yoon J, Lee Y, Quan T, An G. 2016. GL2-Type Homeobox Gene Roc4 in Rice Promotes Flowering Time Preferentially under Long Days by Repressing Gh7. *Plant Science* 252, 133–43.

Xie W, Wang G, Yuan M, Yao W, Lyu K, Zhao H, Yang M, Li P et al. 2015. Breeding signatures of rice improvement revealed by a genomic variation map from a large germplasm collection. *PNAS*, 112 (39), 5411-5419.

Yang M, Lu K, Zhao F, Xie E, Ramakrishna P, Wang G, Du Q, Liang L et al. 2018. Genome-Wide Association Studies Reveal the Genetic Basis of Ionomeric Variation in Rice. *Plant Cell* 30, 2720-2740.

Yang X, Xia X, Zeng Y, Nong B, Zhang Z, Wu Y, et al. 2018. Identification of candidate genes for gelatinization temperature, gel consistency, and pericarp color by GWAS in rice based on SLAF-sequencing. *PLoS ONE* doi:org/10.1371/journal.pone.0196690

Yoshida S, Forno D, Cock JH, Gomez KA. 1976. Determination of Sugar and Starch in Plant Tissue. Laboratory. In: IRRI eds. Manual for Physiological Studies of Rice. Manila Philippines, IRRI, 46–49.

Zhang M, Zhang B, Qian Q, Yu Y, Li R, Zhang J, Liu X, Zeng D, Li J, Zhou Y. 2010. Brittle Culm 12, a Dual-Targeting Kinesin-4 Protein, Controls Cell-Cycle Progression, and Wall Properties in Rice. *Plant Journal* 63 (2), 312–328.

Zhang M, Shan Y, Kochian L, Strasser R, Chen G. 2015. Photochemical Properties in Flag Leaves of a Super-High-Yielding Hybrid Rice and a Traditional Hybrid Rice (*Oryza Sativa* L.) Probed by Chlorophyll a Fluorescence Transient. *Photosynthesis Research* 126(2-3), 275-284.

Zhang N, Yu H, Yu H, Cai Y, Huang L, Xu C, Xiong G, et al. 2018. A Core Regulatory Pathway Controlling Rice Tiller Angle Mediated by the LAZY1-Dependent Asymmetric Distribution of Auxin. *Plant Cell* 30 (7), 1461–1475.

Zhao K, Tung CW, Eizenga G, et al. 2011. Genome-wide association mapping reveals a rich genetic architecture of complex traits in *Oryza sativa*. *Nature Communications* doi: 10.1038/ncomms1467

Tables:

Table 1: Calculations and definitions of fluorescence phenotypes (Strasser *et al.* 2000) and ANOVA analyze of environment (E), genotype (G) and genotype by environment effects on fluorescence phenotypes. Significance of the P-values is given as: *** p< 0.001, **p< 0.01, *p< 0.05, ns (no significance).

Phenotype	calculation	Definition	G	E	GXE
F_o		Minimal fluorescence, when all PSII RCs are open	***	***	***
F_m		maximal recorded fluorescence intensity	***	***	***
F_o/F_m		Relative fluorescence	***	***	***
F_v/F_m	$(F_m - F_o)/F_o$	Maximum efficiency of photochemistry	***	***	***
S_m	$\int_{F_o}^{F_m} (F_m - F_t) dt / F_m - F_o$	Area normalized complementary area related to the number of electron carriers per electron carriers chain or energy needed to close all reaction centers	***	***	***
N	$(Area / (F_m - F_o)) \times M_o \times (1/V_j)$	Turn-over number Qa reduction events between time 0 and F_m	***	***	***
ABS/RC	$M_o \cdot (1/V_j) \cdot (1/TR_o/ABS)$	Energy absorption per reaction center, or size antenna	***	***	***
DI _o /RC	$(ABS/RC) - (TR_o/RC)$	Flux of energy dissipation per reaction center	***	***	***
TR _o /RC	$M_o \cdot (1/V_j)$	Energy flux trapped per reaction center	***	**	***
ET _o /RC	$M_o \cdot (1/V_j) \cdot (ET_o/TR_o)$	Energy flux for electron transport per reaction center	***	***	***
RE _o /RC	$(M_o/V_j) \cdot R_o$	The flux of electrons transferred from Q _a ⁻ to final PSI acceptors per active PSII	***	***	***
$\Psi(E_o)$	ET_o/TR_o	probability that a trapped exciton moves an electron into the electron transport chain beyond Q _a ⁻	***	***	***
$\Phi(E_o)$	ET_o/ABS	Quantum yield for electron transport	***	***	***
$\delta(R_o)$	RE_o/ET_o	Efficiency with which an electron from PQH ₂ transferred to final PSI Acceptors	***	ns	***

$\Phi(R_o)$	RE_o/ABS	Quantum yield of electron transport from Q_a^- to final PSI acceptors	***	***	***
ABS/CS		Energy absorbed per excited cross-section	***	***	***
DI_o/CS	$(ABS/CS_o) - (TR_o/CS_o)$	Flux of energy dissipation per cross-section	***	***	***
TR_o/CS	$(TR_o/ABS) \cdot (ABS/CS)$	Energy flux trapped per cross-section	***	***	*
ET_o/CS	$(TR_o/ABS) \cdot (ET_o/TR_o) \cdot (ABS/CS)$	Energy flux for electron transport per cross-section	***	***	***
RE_o/CS	$(RE_o/ABS) \cdot (ABS/CS)$	The flux of electrons transferred from Q_a^- to final PSI acceptors per cross-section	***	ns	***
RC/(1-RC)	$ChIRC/ChAntenna=RC/ABS$	YRC is the chlorophyll fraction of reaction center and RC/ABS represents the contribution to the PI _{ABS} due to the RC density on a chlorophyll basis.	***	***	***
$\Phi_{po}/(1-\Phi_{po})$	TR_o/DI_o	contribution of the light reactions for primary photochemistry	***	***	***
$\Psi_{Eo}/(1-\Psi_{Eo})$	$ET_o/(TR_o - ET_o)$	contribution of the dark reactions for primary photochemistry	***	***	***
PI_{abs}	$RC/(1-RC) \cdot \Phi_{po}/(1-\Phi_{po}) \cdot \Psi_{Eo}/(1-\Psi_{Eo})$	Performance index (potential) for energy conservation from photons absorbed by PSII to the reduction of intersystem electron acceptors	***	***	***
PI_{total}	$PI_{abs} \cdot \delta_{Ro}/(1-\delta_{Ro})$	Total performance index on absorption basis	ns	ns	ns
DF_{abs}	$\text{Log}(PI_{ABS})$	driving force (DF) or logarithm of the performance index for energy conservation from photons absorbed by PSII to reduction Q_a	***	***	***
Q_bRC	ϕ_p^* / ϕ_{po}	The fraction of QB-reducing reaction	***	***	***
$1-Q_bRC$	$1-Q_b$ reducing center	The fraction of non-QB reducing reaction	***	***	***
SPAD		Chlorophyll content	***	***	***

Table 2: Summary of significative associations between SNP and Chlorophyll Fluorescence phenotypes in the environment CH and ER.

Phenotype	Chromosome	Nº SNP	Environment
F_o/F_m	5	1	CH
F_v/F_m	5	1	CH
DI_o/RC	5	1	CH
DF_{abs}	5	1	CH
δR_o	3, 4, 5, 6, 7, 8	6	CH
PI_{abs}	9	1	CH
F_o/F_m	6	1	ER
F_v/F_m	6	1	ER
S_m	1,2,3,4,5,6,10,12	9	ER
N	1,2,3,4,5,6,7,8,10,11,12	24	ER
ET_o/RC	3,8,11	3	ER
DI_o/RC	1,2,3,4,5,8,10,11,12	24	ER
RE_o/RC	1,2,3,4,5,7	6	ER
DI_o/CS	1,2,3,4,6,8,10,11	10	ER
δR_o	3,6,8,10	5	ER
PI_{abs}	1	1	ER
PI_{total}	2,3,5,6,9	6	ER
Q_b/RC	1,3,4,7,12	8	ER
$1-Q_b/RC$	1	1	ER

Table 3: Enrichment analysis of GO terms based on identified candidate genes: The most statistically representative Go terms are shown.

GO Term	Ontology	Description	Number input list	Number in BG/Ref	p-value
0044249	Molecular Function	Cell Biosynthesis	13	890	$1,40 \times 10^{-6}$
0019222	Molecular Function	Metabolic Regulation Process	6	188	$1,80 \times 10^{-5}$
0010468	Molecular Function	Gene Expression Regulation	6	188	$1,80 \times 10^{-5}$
0060255	Molecular Function	Macromolecular Metabolic Regulation Process	6	188	$1,80 \times 10^{-5}$
0008219	Molecular Function	Cell Death Regulation	8	478	$6,70 \times 10^{-5}$
0034645	Molecular Function	Macromolecule Cell Biosynthesis	9	890	$9,30 \times 10^{-4}$
0009059	Molecular Function	Macromolecules Biosynthesis	9	890	$9,30 \times 10^{-4}$
0016817	Biological Process	Hydrolase activity of anhydrous acid	7	109	$3,80 \times 10^{-8}$
0017111	Biological Process	Nucleoside Phosphatase activity	7	109	$3,80 \times 10^{-8}$
0016818	Biological Process	Hydrolase activity of phosphorous anhydrous acids	7	109	$3,80 \times 10^{-8}$
0016462	Biological Process	Pyrophosphatase activity	7	109	$3,80 \times 10^{-8}$
0000166	Biological Process	Nucleotide-binding	29	3490	$5,50 \times 10^{-8}$
0016788	Biological Process	Hydrolase activity on ester bonds	6	258	$1,00 \times 10^{-4}$

Table 4: Summary of the most important candidate genes identified by GWAS analysis, linked to the most representative Go Terms, Phenotype, Environment, and SNP.

SNP	GO Term	ID	Functional annotation	Environment	Phenotype
SNP-9.16154636	GO: 0000166	LOC_Os09g26620	Auxin repressed protein	CH	Plabs
SNP-5.920701	GO: 0000166	LOC_Os05g02670	Kinesin motor domain protein	CH	$\delta(R_o)$
SNP-10.20737522 SNP-3.11832167 SNP-3.11839954 SNP-3.11840203	GO:0044249	LOC_Os10g39030	Homeobox domain	ER	S_m N DI_o/RC
SNP-5.13606968	GO:0044249	LOC_Os05g23780	OsMADS70 family of genes - MADS-box with expressed M-alpha-type-box	ER	S_m N
SNP-1.32181171	GO:0044249	LOC_Os01g55870	Chloroplast precursor of Corismatemutase	ER	S_m N
SNP-1.32181171	GO:0044249	LOC_Os01g55890	Amino acid kinase	ER	S_m N
SNP-5.26255003. SNP-5.26255003	GO:0044249 GO: 0000166	LOC_Os05g45340 LOC_Os05g45340	ATP binding protein	ER	DI_o/RC
SNP-5.25755857	GO:0044249	LOC_Os05g44360	Oligosaccharide Transferase	ER	DI_o/RC
SNP-3.9505313	GO:0044249	LOC_Os03g17120	Arginine biosynthesis, argJbifunctional protein	ER	Q_bRC
SNP-3.9505313	GO:0044249	LOC_Os03g17130	Transcription factor b Helix-loop-helix	ER	Q_bRC
SNP-5.25752878 SNP-5.25755857	GO:0044249	LOC_Os05g44390	Peptidyl-tRNA hydrolase	ER	DI_o/RC
SNP-5.25752878 SNP-5.25755857	GO:0044249	LOC_Os05g44400	GATA zincfingerdomain	ER	DI_o/RC
SNP-3.11913691 SNP-3.11909250	GO:0044249	LOC_Os03g20970	Phospholipid transporter of type ATPase 1	ER	DI_o/RC
SNP-3.11832167 SNP-3.11840203 SNP-3.11839954	GO:0044249	LOC_Os03g20900	Myb transcription factor	ER	DI_o/RC
SNP-1.672866	GO: 0000166	LOC_Os01g02250	RGA-1	ER	DI_o/RC
SNP-1.2950882	GO: 0000166	LOC_Os01g06240	Protein kinase	ER	DI_o/RC
SNP-1.3777578	GO: 0000166	LOC_Os01g07870	Transporter family protein type A	ER	DI_o/RC
SNP-1.20577084	GO: 0000166	LOC_Os01g36920	ATP-dependent DEAD-box RNA helicase	ER	N $1-Q_bRC$
SNP-1.32181171	GO: 0000166	LOC_Os01g55880	DNA hemimethylated domain-binding protein	ER	S_m N
SNP-2.18755532	GO: 0000166	LOC_Os02g31290	AML1	ER	RE_o/RC S_m N
SNP-3.6370379	GO: 0000166	LOC_Os03g12150	Serine/threonine receptor protein kinase precursor	ER	N

SNP	GO Term	ID	Functional annotation	Environment	Pheno type
SNP-3.33035702	GO: 0000166	LOC_Os03g59600	Mitochondrial RhoGTPase1	ER	DI _o /RC
SNP-3.33935702	GO: 0000166	LOC_Os03g59620	Phospholipase of the patatin family	ER	DI _o /RC
SNP-5.13606968	GO: 0000166	LOC_Os05g23800	Motif for RNA recognition	ER	S _m N
SNP-5.25752878 SNP-5.25755857	GO: 0000166	LOC_Os05g44340	Heat shock protein 101	ER	DI _o /RC
SNP-5.25860213 SNP-5.25870238	GO: 0000166	LOC_Os05g44560	Protein Kinesin motor domain	ER	DI _o /RC
SNP-5.26037406 SNP-5.26067844	GO: 0000166	LOC_Os05g44922	6-phosphofructokinase	ER	DI _o /RC
SNP-5.26037406 SNP-5.26067844	GO: 0000166	LOC_Os05g44930	Protein kinase type receptor	ER	DI _o /RC
SNP-5.26067844	GO: 0000166	LOC_Os05g44940	Protein containing kinase domain	ER	DI _o /RC
SNP-5.26067844	GO: 0000166	LOC_Os05g44970	Senescence receptor precursor of the Serine / Threonine protein kinase type	ER	DI _o /RC
SNP-6.17586886	GO: 0000166	LOC_Os06g30430	RPM1 disease resistance protein	ER	N
SNP-8.17383104	GO: 0000166	LOC_Os08g28470	RPM disease resistance protein	ER	N
SNP-11.9898109	GO: 0000166	LOC_Os09g02400	RNP RNA binding region	ER	DI _o /RC
SNP-9.8690732	GO: 0000166	LOC_Os09g14660	Legume lectins containing beta domain proteins	ER	PI _{total}
SNP-12.1522824	GO: 0000166	LOC_Os12g03750	Leucine-rich protein family in	ER	DI _o /RC
SNP-12.18066755	GO: 0000166	LOC_Os12g30150	CAMK_CAMK_del type 47 - CAMK includes calcium / calmodulin-dependent protein kinases	ER	Q _b RC
SNP-12.18757106 SNP-12.19687181 SNP-12.19687181	GO: 0000166	LOC_Os12g31200 LOC_Os12g32680	Domain that contains NB-ARC	ER	Q _b RC
SNP-12.19687181	GO: 0000166	LOC_Os12g32670	CC-NBS-LRR resistance protein	ER	N

Figure Legends:

Figure 1: Genetic structure of the population: PCA analysis for the first two PCs, the CH environment is represented in light gray and the ER environment is represented in dark gray.

Figure 2: Box plots of fluorescence phenotypes with significant associations in GWAS analysis. The line inside the box represents the mean value of each phenotype, the top and bottom of each represent the 1st and 3rd quartiles. Open circles represent outliers within the dataset. (A). Gray boxes phenotypes corresponding to the environment CH. (B). White boxes phenotypes corresponding to the ER environment.

Figure 3: Manhattan plots for the significant phenotypes found using GWAS for the environment CH. (A). Plots for the F_o/F_m , F_v/F_m , DI_o/RC , and DF_{abs} phenotypes. (B). Plots for the $\delta(R_o)$ and Pl_{abs} phenotypes. The box in red identifies the multi-phenotypic QTL and each SNP is represented by a gray or black dot. The x-axis shows each of the 12 rice chromosomes, the y-axis represents the negative base ten logarithms ($-\log_{10}$) of each p-value corresponding to a particular SNP. The blue line that cuts the y-axis represents the significance threshold value for each SNP.

Figure 4: Manhattan plots for the significant phenotypes found by GWAS for the ER environment. (A). Plots for the F_o/F_m , F_v/F_m , $\delta(R_o)$, DI_o/RC , DI_o/CS , RE_o/RC , N and S_m phenotypes, (B). Plots for the ET_o/RC , Pl_{abs} , Pl_{total} , Q_bRC , and $1 - Q_bRC$ phenotypes (hBN and HIBS). The box in red and the orange dotted line identify multi-phenotypic QTL, green box identifies the multi SNP QTLs, and each SNP is represented by a gray or black dot. The x-axis shows each of the 12 rice chromosomes, the y-axis represents the negative base ten logarithms ($-\log_{10}$) of each p-value corresponding to a particular SNP. The blue line that cuts the y-axis represents the significance threshold value for each SNP.

Figure 5: Box diagram of the analyzed yield components. Gray boxes represent plants grown in the CH environment. White boxes represent plants grown in the ER environment. The line inside the box represents the mean value of each phenotype, the top and bottom of each represent the 1st and 3rd quartiles. Open circles represent outliers within the dataset.

Figure 1: Genetic structure of the population: PCA analysis for the first two PCs, the CH environment is represented in light gray and the ER environment is represented in dark gray.

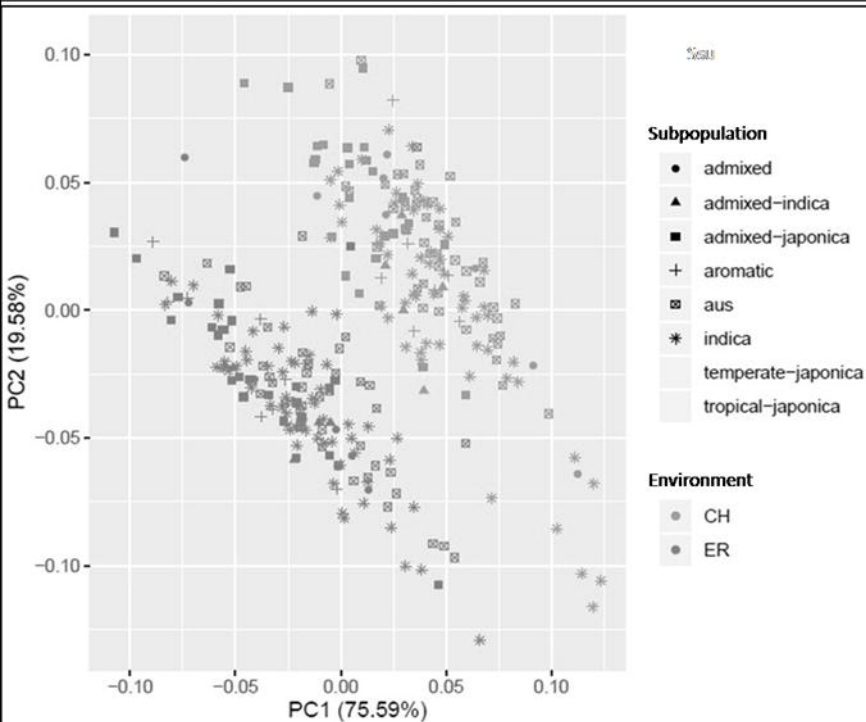
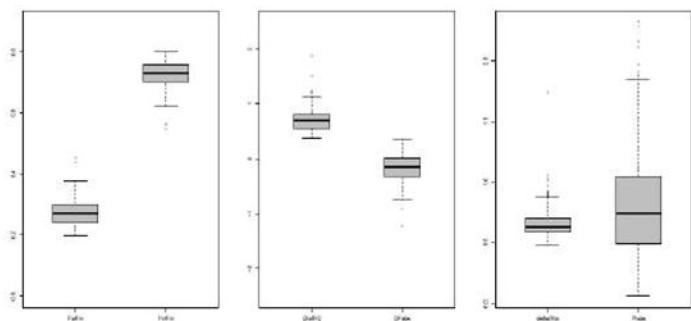


Figure 2: Box plots of fluorescence phenotypes with significant associations in GWAS analysis. The line inside the box represents the mean value of each phenotype, the top and bottom of each represent the 1st and 3rd quartiles. Open circles represent outliers within the dataset. (A). Gray boxes phenotypes corresponding to the environment CH. (B). White boxes phenotypes corresponding to the ER environment.

A



B

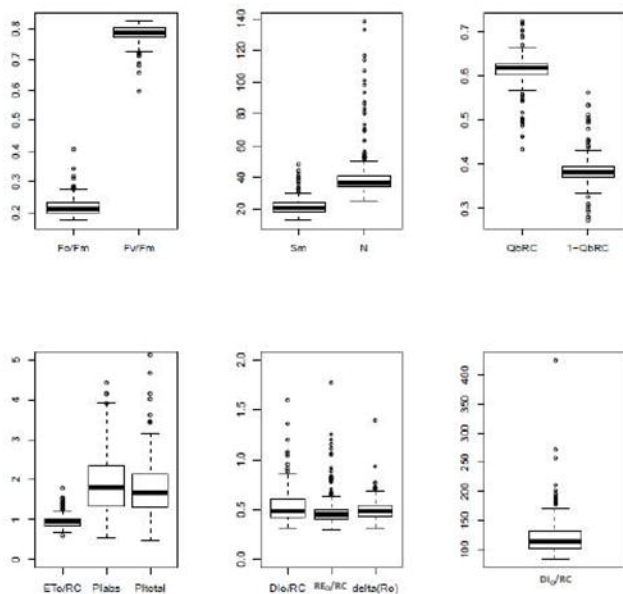


Figure 3: Manhattan plots for the significant phenotypes found using GWAS for the environment CH. (A). Plots for the Fo/Fm, Fv/Fm Dlo/RC, and DFabs phenotypes. (B). Plots for the $\delta(Ro)$ and Plabs phenotypes. The box in red identifies the multi-phenotypic QTL and each SNP is represented by a gray or black dot. The x-axis shows each of the 12 rice chromosomes, the y-axis represents the negative base ten logarithms ($-\log_{10}$) of each p-value corresponding to a particular SNP. The blue line that cuts the y-axis represents the significance threshold value for each SNP.

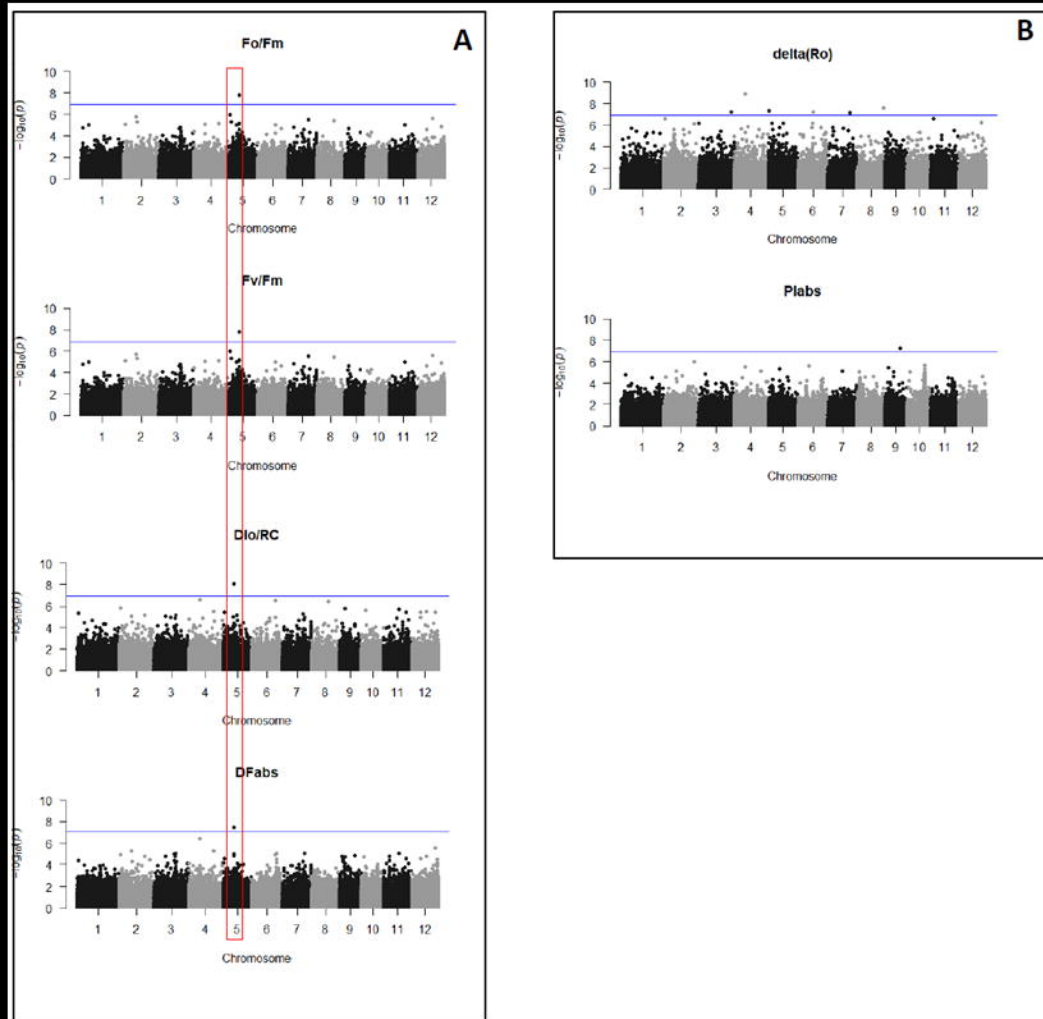


Figure 4: Manhattan plots for the significant phenotypes found by GWAS for the ER environment. (A). Plots for the Fo/Fm, Fv/Fm, $\delta(Ro)$, DIo/RC, DIo/CS, REo/RC, N and Sm phenotypes, (B). Plots for the ETo/RC, PIabs, PItotal, QbRC, and 1- QbRC phenotypes (hBN and HIBS). The box in red and the orange dotted line identify multi-phenotyp QTL, green box identifies the multi SNP QTLs, and each SNP is represented by a gray or black dot. The x-axis shows each of the 12 rice chromosomes, the y-axis represents the negative base ten logarithms ($-\log_{10}$) of each p-value corresponding to a particular SNP. The blue line that cuts the y-axis represents the significance threshold value for each SNP.

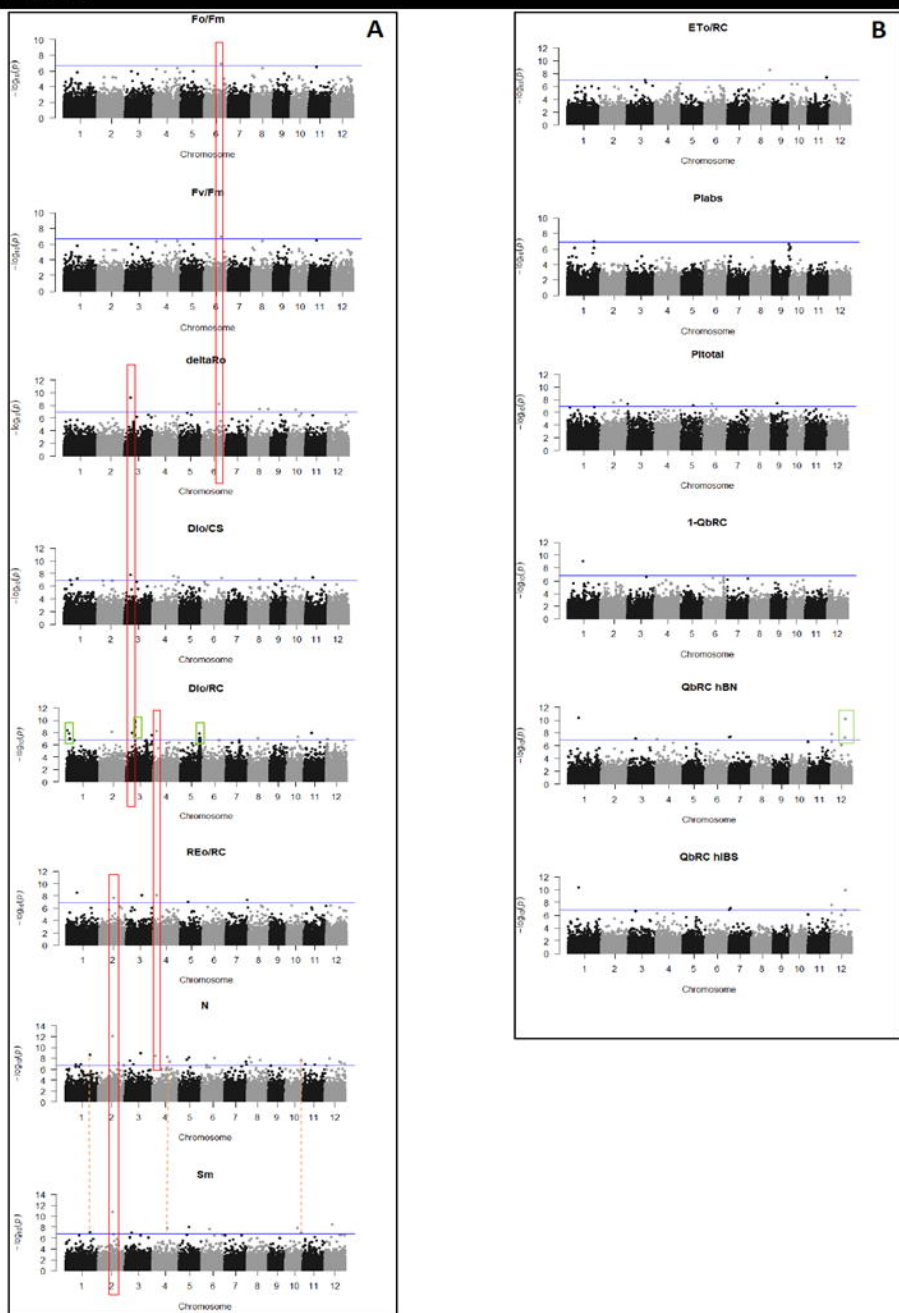


Figure 5: Box diagram of the analyzed yield components. Gray boxes represent plants grown in the CH environment. White boxes represent plants grown in the ER environment. The line inside the box represents the mean value of each phenotype, the top and bottom of each represent the 1st and 3rd quartiles. Open circles represent outliers within the dataset.

